Polarization kinetics of semiconductor microcavities investigated with a Boltzman approach

Huy Thien Cao, T. D. Doan, and D. B. Tran Thoai
Ho Chi Minh City Institute of Physics, Vietnam Center for Natural Science and Technology, 1 Mac Dinh Chi, Ho Chi Minh City, Vietnam

H. Haug
Institut für Theoretische Physik, J.W. Goethe-Universität Frankfurt, Max-von-Laue-Str.1, D-60438 Frankfurt a.M., Germany
(Received 21 February 2007; revised manuscript received 26 September 2007; published 21 February 2008)

We investigate with a Boltzmann approach the spin relaxation kinetics of microcavity polaritons after an excitation pulse with near-resonant polarized light and calculate the polarization of the emitted light around and above the threshold for stimulated emission. Considering only the optically active excitons with an angular momentum $m=\pm 1$, we calculate the corresponding 2×2 single-particle density matrix. Our kinetic treatment takes the polariton-acoustic phonon as well as the polariton-polariton scattering as the dominant relaxation processes into account. Both processes are spin conserving. Particularly for excitation with circular light, we find in isotropic crystals above threshold a nearly complete circular polarization degree which lasts (typically 40–60 ps) much longer than the exciting 3 ps pulses due to the dominance of the stimulated spin-conserving scattering processes over the spontaneous spin-flip processes. These and other results also for linearly polarized pump light are in very good agreement with corresponding experiments on GaAs microcavities. In addition, we present time- and wave-number-dependent results which too are in qualitative agreement with the available angle- and polarization-resolved luminescence measurements.

DOI: 10.1103/PhysRevB.77.075320 PACS number(s): 71.35.Lk, 72.25.Rb, 78.66.−w

I. INTRODUCTION

Semiconductor microcavity (mc) polaritons (p's) are in the low-density regime bosons. The admixture of photons with their ideal bosonic nature to the nonideal excitons (x's) causes an increase in the bosonic nature of the resulting p's, while the interacting x's provide the necessary relaxation processes. The energy of the lower p branch remains finite with a narrow quadratic minimum as the transverse wave-number approaches zero. The p's have been shown to be able to relax toward and condense in the ground state of the lower branch.[1–3] Above a certain critical density, stimulated scattering processes become dominant and result in a finite-size nonequilibrium Bose-Einstein condensation (BEC) in the ground state, which can easily be observed by the onset of coherent laser emission from the mc. It has been seen that the condensation is accompanied by a strong increase of the degree of polarization of the emitted light which can reach values of close to 1.[1–3] This fact makes these semiconductor m's to potential photoelectronic devices with which information encoded in the polarization of light can be processed. Above threshold the rates of the stimulated processes[4] which conserve the x spin are much larger than the rates of the usual spontaneous spin relaxation processes for quantum well x's. Therefore, a stable polarization of the emitted light results. A detailed review of the theory of the x spin Boltzmann kinetics in m's has been given by Shelykh *et al.*.[4] So far, the spin kinetics has been numerically evaluated mainly for the p-acoustic phonon scattering, but the even more important p-p scattering has been omitted,[5] except for two very recent studies mainly concerned with resonant excitation in which the p-p scattering has been included also.[6,7]

In the present paper, we also use the pseudospin formalism in which only the optically active (bright) x's are considered with a total angular momentum of $m=\pm 1$. The reduced single-particle density matrix becomes a 2×2 matrix in this pseudospin index. The diagonal elements describe the population of the two spin states and thus express the circular polarization; the off-diagonal elements describe the in-plane components of the linear polarization. In other words, circular polarization appears as diagonal order and linear polarization as off-diagonal order. The kinetics of the 2×2 density matrix is reminiscent to that of a two-band semiconductor[8] in which the matrix elements off-diagonal in the band index express the optical interband polarization induced by a coherent excitation field.

We obtain the same kinetic equations for the distributions of the two x's in the two spin states and for the polarization field amplitude as Shelykh *et al.*, except for a mean-field term due to the interaction of two p's in the relative singlet state. We solve this set of equations by treating the TE-TM splitting in a so-called cylindrical symmetry approximation[9] numerically using strategies which we have developed for the condensation kinetics of the mc p's disregarding the spin degrees.[10–12] Because the considered p's have to be excited optically, undergo a dissipative relaxation, and finally decay again, one has to treat the bosonic condensation in the framework of nonequilibrium phase transitions with concepts developed in the theory of lasers and synergetics.[13] mc photons and quantum well x's have only transverse translational degrees of freedom; therefore, it is important to take explicitly the finite cross section of the semiconductor mc into account. The finite geometry discretizes the transverse momentum components and, in particular, introduces a gap between the ground state and the excited states. With this gap a finite-size BEC of the two-dimensional (2D) p gas is obtained for nonzero temperatures of the p gas. We have shown[10–12] that the ground state population has to be treated separately from the higher levels which can approximately be treated as an excitation continuum. We follow here this concept by considering the population and the polarization components of the ground state separately from the distributions of these vari-

ables over the excited state. We calculate the spin kinetics for GaAs mc's without considering any crystal anisotropy which has to be included for II-VI compound m's.[2,6,14,15] Furthermore, detailed experimental observations are available for GaAs m's[1,3] with which we will compare our numerical results.

II. FORMULATION OF THE SPIN KINETICS

It is important for the p spin kinetics to include the TE-TM splitting for the p's with the pseudospin components $i=+1$ and $i=-1$.[4] As in our previous treatments, we include the interactions of the p's via their x component with the acoustic phonons and the p-p interaction in the relative triplet states as well as in the relative singlet states of their pseudospins. These p-p interactions stem from the Coulomb interactions between the electrons and holes of the x components calculated with the relative x wave functions belonging to a specific spin state. In order to study the distribution and spin kinetics, we have to calculate the single-particle density matrix. For a spatially homogeneous system, the density matrix is a 2×2 matrix in the spin index and diagonal in the 2D k space,

$$\rho_{k,ij}(t) = \langle b^{\dagger}_{k,j}(t) b_{k,i}(t) \rangle, \tag{1}$$

where $b_{k,i}(t)$ is the annihilation operator of a p with transverse momentum k (we suppress the vector symbols of k to ease the notation) and with pseudospin $i=\pm 1$. The 2×2 matrix in the spin index can be composed conveniently using a unit matrix I and the Pauli spin matrices σ^l_{ij}, where the upper index runs over the space directions x,y,z,

$$\rho_{k,ij}(t) = \frac{N_k(t)}{2}\delta_{ij} + \sum_l S^l_k(t)\sigma^l_{i,j}, \tag{2}$$

with the Pauli matrices

$$\sigma^x = \begin{pmatrix} 0 & 1 \\ 1 & 0 \end{pmatrix}, \quad \sigma^y = \begin{pmatrix} 0 & -i \\ i & 0 \end{pmatrix}, \quad \sigma^z = \begin{pmatrix} 1 & 0 \\ 0 & -1 \end{pmatrix}.$$

The diagonal elements yield with the distribution functions $\rho_{k,ii}(t)=f_{k,i}(t)$,

$$N_k(t) = \sum_i f_{k,i}(t) \tag{3}$$

and

$$S^z_k(t) = \frac{1}{2}[f_{k,1}(t) - f_{k,2}(t)]. \tag{4}$$

The off-diagonal elements determine the x and y components of the polarization amplitude,

$$S^x_k(t) = \frac{1}{2}[\rho_{k,12}(t) + \rho_{k,21}(t)], \tag{5}$$

and

$$S^y_k(t) = \frac{i}{2}[\rho_{k,12}(t) - \rho_{k,21}(t)]. \tag{6}$$

The Hamiltonian of the system is given by

$$\begin{aligned} H = & \sum_{k,s} e_k b^{\dagger}_{k,s} b_{k,s} + \frac{1}{2}\sum_k (\Omega_k b^{\dagger}_{k,1} b_{k,2} + \text{H.c.}) + \sum_{q,q_z} \omega_{q,q_z} a^{\dagger}_{q,q_z} a_{q,q_z} \\ & + \sum_{k,q,q_z,s} G(k,q,q_z)(a^{\dagger}_{q,q_z} + a_{-q,q_z}) b^{\dagger}_{k+q,s} b_{k,s} \\ & + \frac{1}{4}\Bigg\{ \sum_{k,k',q,s} V(k+q,k'-q,k,k')(b^{\dagger}_{k,s} b^{\dagger}_{k',s} b_{k'-q,s} b_{k+q,s}) \\ & + \sum_{k,k',q,s\neq s'} U(k+q,k'-q,k,k')(b^{\dagger}_{k,s} b^{\dagger}_{k',s'} b_{k'-q,s'} b_{k+q,s} \\ & + b^{\dagger}_{k,s} b^{\dagger}_{k',s'} b_{k'-q,s} b_{k+q,s'}) + \text{H.c.} \Bigg\}, \end{aligned} \tag{7}$$

where $a^{\dagger}_{q,q_z}$ and a_{q,q_z} are the generation and annihilation operators of the acoustic phonons, respectively. e_k is the dispersion of the lower p branch. Ω_k is a complex energy, related to the TE-TM splitting. ω_{q,q_z} is the frequency of the acoustic phonon, with the in-plane wave number q and the wave number q_z perpendicular to the quantum well layers. The p-phonon coupling constant $G(k,q,q_z)$ is given by[16]

$$G(k,q,q_z) = i\sqrt{\frac{\hbar(|q|^2+q_z^2)^{1/2}}{2\rho V u}} B(q_z) D(|q|) u_k u^*_{k+q}. \tag{8}$$

Here, u_k (v_k) are the x (photon) Hopfield coefficients of the lower branch p's.[10,11,18,19] The weighted Fourier transforms of the 2D x wave function are

$$D(|q|) = D_e F\left(\frac{|q|m_h}{M}\right) - D_h F\left(\frac{|q|m_e}{M}\right), \tag{9}$$

with

$$F(q) = [1 + (qa_B/2)^2]^{-3/2}, \tag{10}$$

and the e(h)-structure factors are given by

$$B(q_z) = \frac{8\pi^2}{q_z L(4\pi^2 - q_z^2 L^2)} \sin\left(\frac{q_z L}{2}\right), \tag{11}$$

where $D_{e(h)}$ are the electron and hole deformation potentials and L is the quantum well width.

The matrix elements $V(k,k',k'-q,k+q)$ and $U(k,k',k'-q,k+q)$ describe scattering of p's in the relative triplet and singlet configurations, respectively. They are given by[4]

$$V(k,k',k'-q,k+q) = 6E_B a_B^2 u_{k+q} u_{k'-q} u_{k'} u_k,$$

$$U(k,k',k'-q,k+q) = -\alpha V(k,k',k'-q,k+q), \quad \alpha > 0,$$

$$\begin{aligned} T(k,k',k'-q,k+q) = & V(k,k',k'-q,k+q) \\ & \times U(k,k',k'-q,k+q), \end{aligned} \tag{12}$$

where E_B and a_B are the binding energy and Bohr radius of the exciton in 2D, respectively. With the x and y components, we define a 2D polarization vector,

$$\vec{S}_k = (S^x_k, S^y_k), \tag{13}$$

$$2\vec{S}_k\vec{S}_{k'} = \rho_{k,21}\rho_{k',12} + \rho_{k,12}\rho_{k',21}. \tag{14}$$

Similarly, we decompose the TE-TM splitting into x and y components which form again an effective 2D magnetic field (we absorb the g factor and magnetic moment in this effective field),

$$\Omega_k = \Omega_k^x + i\Omega_k^y,$$

$$\vec{\Omega}_k = (\Omega_k^x, \Omega_k^y), \tag{15}$$

where the components of the splitting field have been given by[9,17] as

$$\Omega_k^x = \Omega_k \frac{k_x^2 - k_y^2}{k^2} = \Omega_k \cos(2\phi),$$

$$\Omega_k^y = \Omega_k \frac{2k_x k_y}{k^2} = \Omega_k \sin(2\phi), \tag{16}$$

where ϕ is the polar angle of the in-plane momentum vector, i.e., $k_x = k\cos(\phi)$ and $k_y = k\sin(\phi)$. The momentum dependence of the splitting field [Eq. (16)] is due to the TE-TM mc modes, together with the momentum dependences of the optical matrix elements of the L and T x's. From the equations of the motion, we get the kinetic equations of the spin i polariton distribution function $f_{k,i}$ and in-plane pseudospin $\vec{S}_k$,

$$\frac{\partial f_{k,j}}{\partial t} = -\frac{f_{k,j}}{\tau_k} + \left.\frac{\partial f_{k,j}}{\partial t}\right|_{S\text{-}F} + \left.\frac{\partial f_{k,j}}{\partial t}\right|_{mf\text{-}s\text{-}s} + \left.\frac{\partial f_{k,j}}{\partial t}\right|_{scatt}^{p\text{-}ph} + \left.\frac{\partial f_{k,j}}{\partial t}\right|_{scatt}^{p\text{-}p} + \frac{1}{2}p_j P(k,t), \quad j = 1,2, \tag{17}$$

where the changes due to the splitting field are given by

$$\left.\frac{\partial f_{k,j}}{\partial t}\right|_{S\text{-}F} = -\frac{1}{\hbar}(-1)^j \vec{e}_z[\vec{S}_k \times \vec{\Omega}_k]. \tag{18}$$

The mean-field term due to the interaction of singlet p's is given by

$$\left.\frac{\partial f_{k,j}}{\partial t}\right|_{mf\text{-}s\text{-}s} = \frac{2}{\hbar}(-1)^j \sum_q U(k,q,k,q)[\vec{S}_k \times \vec{S}_q]. \tag{19}$$

This term due to singlet-singlet interaction [Eq. (19)] which follows directly from the Heisenberg equations for the p operators is absent in the original formulation of Shelykh *et al.*[4]

$$\frac{\partial \vec{S}_k}{\partial t} = -\frac{\vec{S}_k}{\tau_{ks}} + \left.\frac{\partial \vec{S}_k}{\partial t}\right|_{S\text{-}F} + \left.\frac{\partial \vec{S}_k}{\partial t}\right|_{mf\text{-}p\text{-}p} + \left.\frac{\partial \vec{S}_k}{\partial t}\right|_{scatt}^{p\text{-}ph} + \left.\frac{\partial \vec{S}_k}{\partial t}\right|_{scatt}^{p\text{-}p} + \frac{1}{2}\vec{e}_p P(k,t) \tag{20}$$

Here, the mean-field term due to the p-p interaction is

$$\left.\frac{\partial \vec{S}_k}{\partial t}\right|_{mf\text{-}p\text{-}p} = \frac{2}{\hbar}\sum_q [V(k,q,k,q) - U(k,q,k,q)](f_{q,1} - f_{q,2}) \times [\vec{e}_z \times \vec{S}_k], \tag{21}$$

where $\vec{e}_z$ is the unit vector in the direction of the structure growth axis, p_j and $\vec{e}_p$ denote the components of the pump polarization in z direction and (x,y) plane, respectively. $p_1 = 2$ and $p_2 = 0$ for the circular pump and $p_1 = p_2 = 1$ for the linear pump. The changes of the in-plane polarization due to the splitting field are given by

$$\left.\frac{\partial \vec{S}_k}{\partial t}\right|_{S\text{-}F} = \frac{1}{\hbar}\left(\frac{f_{k,1} - f_{k,2}}{2}\right)\vec{e}_z \times \vec{\Omega}_k. \tag{22}$$

For the strength of the TE-TM splitting field Ω_k, we take the numerically determined values of Shelykh *et al.*[4]

τ_k is the p lifetime. The pump rate will be taken in the form[11]

$$P(k,t) = P_0 e^{-[\hbar^2(k-k_p)^2]/2m_x\Delta E} e^{-2\ln 2(t/t_p)^2}, \tag{23}$$

which describes a near-resonant pump rate around the wavenumber k_p with a certain energy width ΔE and in time a Gaussian pulse with a pulse width t_p. The p lifetime τ_k is given[11,12,18] by the cavity lifetime times the photon Hopfield coefficient up to the wavenumber k_c, where the Bragg mirrors become transparent. Above k_c, the losses are given by the radiative losses of the quantum well x's into the radiation continuum. Finally, above, k_{rad}, the quantum well x's decouple from the radiation field, so that in this region $1/\tau_k = 0$. The in-plane pseudospin lifetime will be estimated as $\tau_{ks}^{-1} = \tau_k^{-1} + \tau_{sl}^{-1}$, where τ_{sl} is the characteristic time of the spin-lattice relaxation.

In the Markov approximation, the scattering terms in Eqs. (17) and (20) are given by

$$\left.\frac{\partial f_{k,i}}{\partial t}\right|_{scatt}^{p\text{-}ph} = -\frac{2\pi}{\hbar}\sum_{k'}\{W_{k',k}(f_{k,i}(1+f_{k',i}) + \vec{S}_k\vec{S}_{k'}) - W_{k,k'}(f_{k',i}(1+f_{k,i}) + \vec{S}_k\vec{S}_{k'})\}, \tag{24}$$

$$\left.\frac{\partial \vec{S}_k}{\partial t}\right|_{scatt}^{p\text{-}ph} = -\frac{2\pi}{\hbar}\sum_{k'}\left\{W_{k',k}\left(\vec{S}_k + \frac{1}{2}\sum_{i=1,2}(f_{k',i}\vec{S}_k + f_{k,i}\vec{S}_{k'})\right) - W_{k,k'}\left(\vec{S}_{k'} + \frac{1}{2}\sum_{i=1,2}(f_{k,i}\vec{S}_{k'} + f_{k',i}\vec{S}_k)\right)\right\}, \tag{25}$$

$$\left.\frac{\partial f_{k,i}}{\partial t}\right|_{scatt}^{p\text{-}p} = -\frac{2\pi}{\hbar}\sum_{k',q}\Bigg[\delta(e_{k'-q}+e_{k+q}-e_k-e_{k'})$$
$$\times\Bigg(|V(k,k',k'-q,k+q)|^2[f_{k,i}f_{k',i}(1+f_{k'-q,i}+f_{k+q,i})-f_{k'-q,i}f_{k+q,i}(1+f_{k,i}+f_{k',i})]$$
$$+|U(k,k',k'-q,k+q)|^2\Bigg[(f_{k,i}f_{k',\bar{i}}+\vec{S}_k\vec{S}_{k'})\Bigg(2+\sum_{j=1,2}(f_{k'-q,j}+f_{k+q,j})\Bigg)$$
$$-(1+f_{k,i}+f_{k',\bar{i}})\Bigg(2\vec{S}_{k'-q}\vec{S}_{k+q}+\sum_{j=1,2}f_{k'-q,\bar{j}}f_{k+q,j}\Bigg)\Bigg]$$
$$+T(k,k',k'-q,k+q)\Bigg\{\sum_{j=1,2}[(f_{k',j}-f_{k'-q,j})\vec{S}_{k+q}\vec{S}_k+(f_{k',j}-f_{k+q,j})\vec{S}_{k'-q}\vec{S}_k]$$
$$+2[f_{k,i}(\vec{S}_{k'}\vec{S}_{k'-q}+\vec{S}_{k'}\vec{S}_{k+q})-f_{k'-q,i}\vec{S}_{k'}\vec{S}_{k+q}-f_{k+q,i}\vec{S}_{k'}\vec{S}_{k'-q}]\Bigg\}\Bigg)\Bigg], \tag{26}$$

$$\left.\frac{\partial \vec{S}_k}{\partial t}\right|_{scatt}^{p\text{-}p} = -\frac{\pi}{\hbar}\sum_{k',q}\Bigg[\delta(e_{k+q}+e_{k'-q}-e_k-e_{k'})$$
$$\times\Bigg(|V(k,k',k'-q,k+q)|^2\Bigg(\vec{S}_k\sum_{i=1,2}[f_{k',i}(1+f_{k'-q,i}+f_{k+q,i})-f_{k'-q,i}f_{k+q,i}]$$
$$-2[\vec{S}_{k+q}(\vec{S}_{k'}\vec{S}_{k'-q})+\vec{S}_{k'-q}(\vec{S}_{k'}\vec{S}_{k+q})-\vec{S}_{k'}(\vec{S}_{k'-q}\vec{S}_{k+q})]\Bigg)$$
$$+|U(k,k',k'-q,k+q)|^2\Bigg[\sum_{i=1,2}(\vec{S}_kf_{k',i}+\vec{S}_{k'}f_{k,i})\Bigg(2+\sum_{i=1,2}(f_{k'-q,i}+f_{k+q,i})\Bigg)$$
$$-2(\vec{S}_k+\vec{S}_{k'})\Bigg(\sum_{i=1,2}(f_{k'-q,i}f_{k+q,\bar{i}})+2\vec{S}_{k'-q}\vec{S}_{k+q}\Bigg)\Bigg]$$
$$+T(k,k',k'-q,k+q)\Bigg\{4\vec{S}_k(\vec{S}_{k'}\vec{S}_{k'-q}+\vec{S}_{k'}\vec{S}_{k+q})+\vec{S}_{k'-q}\Bigg[\sum_{i=1,2}f_{k,i}\Bigg(\sum_{i=1,2}(f_{k',i}-f_{k+q,i})\Bigg)-2\sum_{i=1,2}f_{k+q,i}(1+f_{k',i})\Bigg]$$
$$+\vec{S}_{k+q}\Bigg[\sum_{i=1,2}f_{k,i}\Bigg(\sum_{i=1,2}(f_{k',i}-f_{k'-q,i})\Bigg)-2\sum_{i=1,2}f_{k'-q,i}(1+f_{k',i})\Bigg]\Bigg\}\Bigg)\Bigg], \tag{27}$$

where

$$W_{k',k}=\begin{cases}|G(k,k'-k)|^2N_{k'-k}\delta(e_{k'}-e_k-\hbar\omega_{k'-k}), & |k'|>|k|\\ |G(k,k'-k)|^2(N_{k'-k}+1)\delta(e_{k'}-e_k-\hbar\omega_{k'-k}), & |k'|<|k|.\end{cases} \tag{28}$$

As a simplifying approximation, we use the assumption of a cylindrical symmetry which has been introduced in Ref. 9, in which the polarization has a only radial component $\vec{S}_k = S_k^r\vec{e}_r$ and in which the splitting field is taken to be orthogonal to the polarization vector. This assumption does not hold in general, so that with the cylindrical symmetry assumption certain directional properties of the splitting field are not correctly taken into account. Because the effects of the splitting field are with respect to the presently investigated aspects of the spin kinetics relatively small, we believe that this inaccuracy can be accepted in a first approach to the problem. Using this cylindrical symmetry, we obtain the following set of equations for $f_{k,j}$ and the radial component S_k^r of the in-plane spin polarization:

$$\frac{\partial f_{k,j}}{\partial t} = -\frac{f_{k,j}}{\tau_k}+\left.\frac{\partial f_{k,j}}{\partial t}\right|_{S\text{-}F}+\left.\frac{\partial f_{k,j}}{\partial t}\right|_{scatt}^{p\text{-}ph}+\left.\frac{\partial f_{k,j}}{\partial t}\right|_{scatt}^{p\text{-}p}$$
$$+\frac{1}{2}p_jP(k,t),\quad j=1,2, \tag{29}$$

$$\frac{\partial S_k^r}{\partial t} = -\frac{S_k^r}{\tau_{ks}}+\left.\frac{\partial S_k^r}{\partial t}\right|_{S\text{-}F}+\left.\frac{\partial S_k^r}{\partial t}\right|_{scatt}^{p\text{-}ph}+\left.\frac{\partial S_k^r}{\partial t}\right|_{scatt}^{p\text{-}p}$$
$$+\frac{1}{2}|\vec{e}_p|P(k,t), \tag{30}$$

where the splitting field terms reduce to

$$\left.\frac{\partial f_{k,j}}{\partial t}\right|_{S\text{-}F} = -\frac{1}{\hbar}(-1)^j S_k^r \Omega_k, \tag{31}$$

and

$$\left.\frac{\partial S_k^r}{\partial t}\right|_{S\text{-}F} = \frac{1}{\hbar}\left(\frac{f_{k,1}-f_{k,2}}{2}\right)\Omega_k. \tag{32}$$

The mean-field terms due to p-p interaction [Eqs. (19) and (21)] vanish in the cylindrical approximation due to the angle integration.

The scattering terms in Eqs. (29) and (30) in the cylindrical approximation are given in the appendix. Apart from the p-p scattering terms, which are new here, Eqs. (29) and (30) coincide with Eqs. (15)–(17) by Kavokin *et al.*[9]

In this form of the rate equations, the necessity to keep the cross section S finite has two reasons: First, only with a finite S a well-defined condensation occurs,[10] and second only with a finite S the spontaneous transition rates into the condensate are maintained which initiate the condensation.[20] Again the separation of the transitions between the continuum and the condensate has to be performed as before (for details see Ref. 10).

Before we present results, we list the used material parameters for GaAs-type quantum wells and mc's:[10,11,18,21,22] $E_0^x=1.515$ eV, $m_e=0.067m_0$, $m_h=0.45m_0$, $a_{2D}=10$ nm, the index of refraction $n_{cav}=3.43$, the cavity Rabi splitting $\hbar\Omega=5$ meV, the deformation potentials $D_e=-8.6$ eV, $D_h=3.5$ eV, $u=4.81\times10^5$ cm/s, and $\rho=5.3\times10^3$ kg/m^3. The mc cross section will be taken as $S=100$ μm^2 and the quantum well width as $L_z=5$ nm. The lifetimes are assumed to be $\tau^x=30$ ps, $\tau^c=2$ ps, and $\tau_{sl}=15$ ps. The smallness parameter of the interaction between excitons in the relative singlet state is $\alpha=5\times10^{-2}$. The bath temperature is $T=4$ K. As in the experiment of Deng *et al.*,[1] the detuning between the cavity mode and the x resonance will be assumed to be zero. The pumping width is $\Delta E=0.1$ meV. The pumping is centered at $k_p=1.7\times10^5$ cm^{-1}. The pump pulse width is as in the experiment,[1] $t_p=3$ ps.

III. NUMERICAL RESULTS

A. Time-averaged results

First, we will examine the time-averaged ground state density for a pump pulse with circularly polarized light as it has been measured by Deng *et al.*[1] Here, we use the total number of excited p's as a measure of the pump power. As expected, the population of p's with cocircular polarization exhibit a clear condensation threshold [solid line in Fig. 1(a)], while the ground state density of the p's with cross-circular polarization [dashed line in Fig. 1(a)] stays subcritical up to a total p density of 10^{11} cm^{-2}, where it is about 4 orders of magnitude smaller than the cocircular density.

Next, we calculate the ground state p densities for left- and right-circular polarizations when the mc has been excited with a linearly polarized light pulse. Figure 1(b) shows that due to the TE-TM splitting, the ground state population for the left-circular p's (solid line) has a lower threshold generation rate, while the right-circular p's also condense but

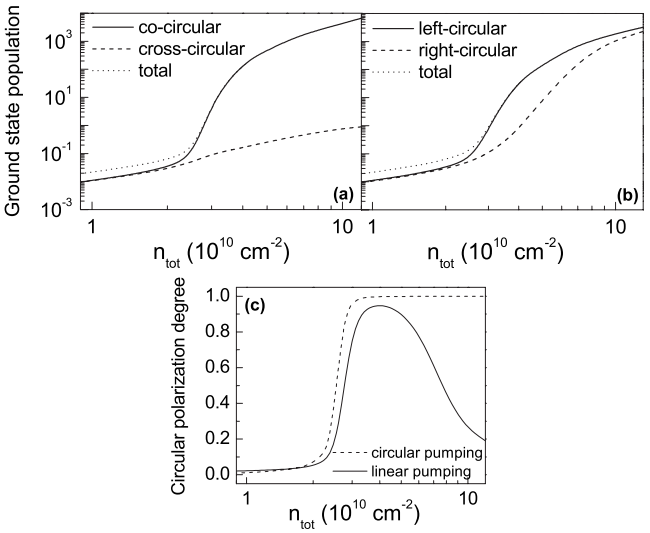

FIG. 1. Ground state density for the lower p's versus total p density under pumping (a) with circularly polarized (b) with linearly polarized light at $T=4$ K in a GaAs mc. The sum of the ground state densities is given by the dotted line, the spin-up p density by the solid line, and the spin-down density by the dashed line. (c) Circular polarization degree of light emitted from the ground state. For linearly polarized pumping, the light intensity is given by the solid line, and for circularly polarized pumping by the dashed line

at a generation rate which is about a factor of 3 higher than those of the left-circular p's. At the highest generation rates, the ground state populations of both circular polarizations approach each other. Finally, we plot in Fig. 1(c) the circular polarization degree, i.e., the normalized difference between the ground state populations of the left- and right-circular p's for circularly and linearly polarized pump light. For circular pump, the polarization degree increases rapidly at the condensation threshold and approaches a value close to 1. For linearly polarized pumping, the polarization degree increases to a value of about 0.95 but decreases rapidly when the right-circular p's condense and approach a value close to zero at the highest pump rates. The comparison of the experimental results (see Fig. 2) with our calculated results of Fig. 1 shows a very good qualitative agreement. In particular, the absence of a threshold for the cross-polarized p's for circular pumping shown in Figs. 1(a) and 2(a) is present in both theory and experiment. Similarly, the successive condensations of the left- and right-circular p's separated by about a factor of 3 in the corresponding threshold generation rates in Figs. 1(b) and 2(b) agrees well. Finally, the polarization degree for circular pumping remains high in both theory and experiment [see Figs. 1(c) and 2(c)], while the polarization degree for linearly polarized pumping decreases again about three to four times above the threshold generation rate.

Shelykh *et al.*[5] have also solved numerically the polarization kinetics for the p-phonon and the p-electron scattering, but not for the p-p scattering. If one compares nevertheless the results of their and our studies, one sees that Shelykh *et al.* obtain for linear pump polarization only a polarization degree of 0.6, while we find [see Fig. 1(c)] in agreement with the experiment [see Fig. 2(c)] values close to 1. Furthermore,

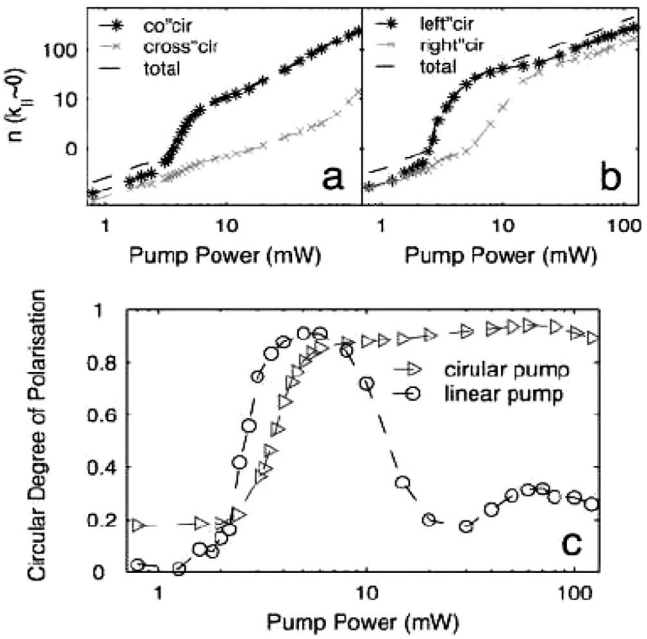

FIG. 2. For comparison the measured time-averaged polarization properties of a GaAs mc of Deng *et al.* (Ref. 1) is shown. (a) Emitted light intensity of the polariton ground state for circularly polarized and (b) for linearly polarized pump light. (c) The circular degree of polarization is plotted for pumping with linear and circular polarizations

the calculated threshold densities of Ref. 5 ($>1 \times 10^{11}$ cm^{-2}) are about 1 order of magnitude higher than ours. Finally, if we compare for circular pumping the results of Shelykh *et al.*[5] with Fig. 1(a) and with the experiment [Fig. 2(a)], it is obvious that their cross-circular polarization component increases too much. This shows that in the present studies considerable progress toward a more quantitative description of the polarization kinetics has been made.

B. Time-resolved results

Here, we will show how populations and polarization develop in time after the excitation with a circularly polarized 3 ps pump pulse. In Fig. 3(a), we show the buildup and decay of the ground state populations with left- and right-circular polarizations for a subcritical pump pulse strength. It is seen that the populations of both spin states reach a maximum between 20 and 30 ps and decay from this point jointly. For a supercritical circularly polarized pump pulse, the temporal evolution of the ground state populations for spin up and spin down is shown in Fig. 3(b). Here, the degenerate spin-up state population exceeds over a long time period (up to 80 ps) the population of the spin-down state which increases much slower. After 80 ps, both populations have become subcritical and decay jointly.

In Fig. 4, the calculated time evolution of the polarization degree for circular pump is shown for various total p densities. Again, it is seen that the polarization degree approaches values close to 1 very fast for supercritical pumping and last longer for increasing pumping. Particularly striking is the different time evolution for the subcritical and supercritical

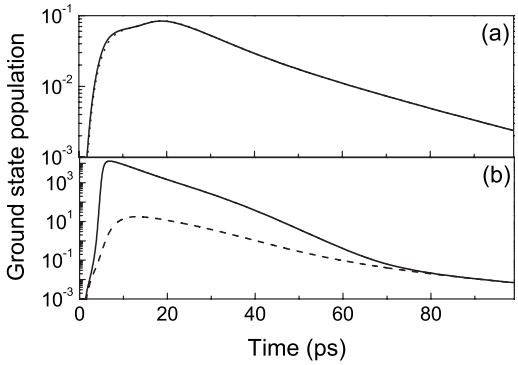

FIG. 3. Time dependence of the ground state populations for spin up (full line) and spin down (doted line) for a circularly polarized near-resonant 3 ps (a) subcritical pump pulse which excites $N_{tot}=1.62\times10^{10}$ cm^{-2} and (b) a supercritical pump pulse which excites $N_{tot}=4.63\times10^{10}$ cm^{-2}.

excitations, as well as the trends of a longer lasting polarization degree with increasing pumping. Below threshold, the polarization degree decays rapidly. Above the threshold, the polarization degree remains close to one followed by a steep decay. The decay time increases with increasing pump strength in the shown examples from about 30 ps to about 70 ps. Similar results for the polarization degree are contained in the preprint of Solnyshkov *et al.*[7]

The calculated scenario of the kinetics of the polarization degree can be compared with corresponding measurements shown in Fig. 5 of Renucci *et al.*[3] in GaAs mc's, where, however, a resonant excitation has been used.

One sees also here an immediate decay of the polarization degree for below-threshold excitation. Above threshold, the experiment also finds the characteristic plateau of the polarization degree with values close to 1, followed by a decay with decay times (between 70 and 90 ps) which increase with increasing pump strength.

Finally, we want to show in Fig. 6 the radial component S_0^r of the spin polarization for a linearly polarized pump which excites a total p density of $N_{tot}=1.63\times10^{10}$ cm^{-2} (solid line) and $N_{tot}=4.63\times10^{10}$ cm^{-2} (dashed line), respectively. S_0^r reaches its maximal value right after the pulse and

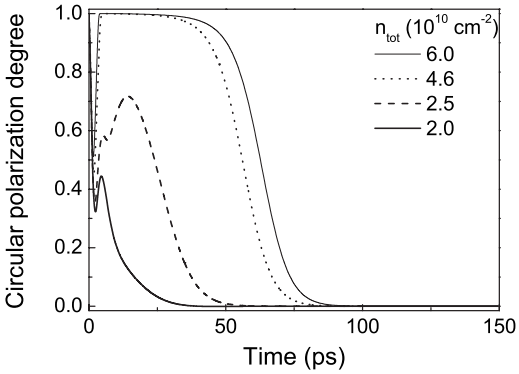

FIG. 4. Calculated time dependence of the circular polarization degree for circularly polarized near-resonant 3 ps pump pulses which excite a total p density of $N_{tot}=2.0$, 2.5, 4.6, and 6.0 $\times10^{10}$ cm^{-2}.

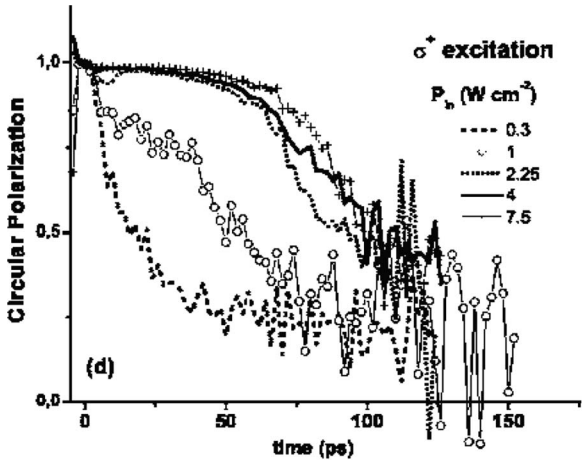

FIG. 5. Measured time dependence of the circular polarization degree for circularly polarized pump pulses in GaAs mc's according to Renucci *et al.* (Ref. 3).

decays rapidly in times of about 20 ps both below (full line) and above threshold (dashed line).

C. Polarization distributions in *k* space

The polarization of the emitted light can be observed not only for the ground state but with angle-resolved luminescence measurements also for the higher k-states. Therefore, we will present in this section the wave-number dependence of the populations and of the radial component of spin polarization $S_k^r(t)$ for various excitation conditions. In Fig. 7, we present for a circularly polarized pump pulse the distribution of the spin-up p's (a) below condensation threshold and (b) above condensation threshold. While below threshold the relaxation into a Maxwell-Boltzmann distribution is still incomplete after 20 ps, one sees that above threshold degenerate distributions are established in the first 10 ps.

For a linearly polarized pump pulse, we show in Fig. 8 the distribution of the radial component $S_k^r(t)$ of the spin polarization for various times. It is seen that this distribution too relaxes slowly below threshold, and much faster above

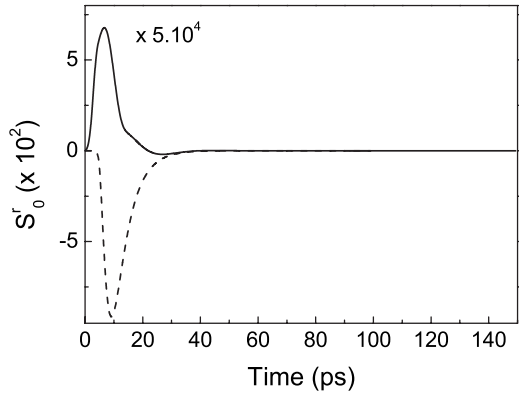

FIG. 6. Calculated time dependence of S_0^r under linearly polarized near-resonant 3 ps pump pulses which excite a below threshold density of $n_{tot}=1.63\times10^{10}$ cm^{-2} (solid line) and above threshold density of $n_{tot}=4.63\times10^{10}$ cm^{-2} (dashed line).

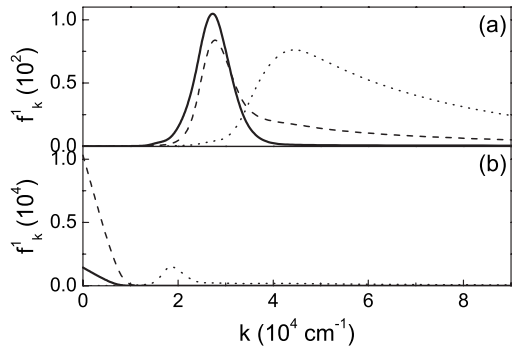

FIG. 7. Calculated wave-number and time dependences of the spin-up p distribution $f_k^1(t)$ for circularly polarized near-resonant 3 ps subcritical and supercritical pump pulses which excite (a) $N_{tot}=1.62\times10^{10}$ cm^{-2} for $t=6$ ps (dotted line), $t=12$ ps (dashed line), and $t=20$ ps (solid line) and (b) $N_{tot}=4.63\times10^{10}$ cm^{-2} for $t=4$ ps (dotted line), $t=9$ ps (dashed line), and $t=20$ (solid line) ps, respectively.

threshold, where its spectrum extends already after a few picoseconds toward the lowest k states.

In order to be able to compare also the polarization of the finite-momentum states with corresponding experimental observations, we show the pump-power dependence of the time-averaged population of three momentum states which are observable under the emission angles $\theta=3°$, 6°, and 9° for circularly and linearly polarized pumpings in the left and right parts of Fig. 9, respectively.

As expected the population of the cocircular polarization exceeds above threshold for all momenta those of the cross-circular polarization strongly. For linearly polarized pumping (right parts of Fig. 9), the difference between the populations of left- and right-hand circular polarizations is considerably smaller. The difference increases slightly with increasing pump power and emission angle, respectively. See Fig. 10

For comparison with the experiment, we show the results of Deng *et al.* for the angle- and polarization-resolved luminescence of the GaAs mc's, plotted in Fig. 9.

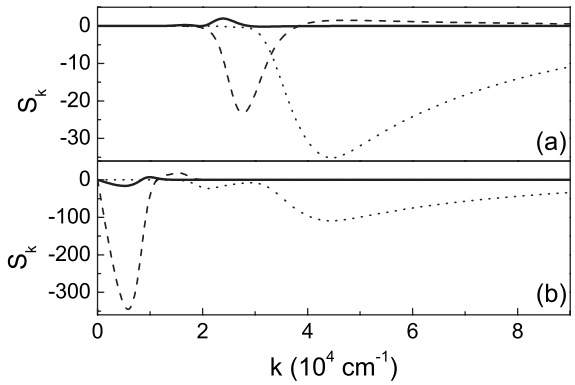

FIG. 8. Calculated time dependence of the radial component of the linear polarization, $S_k^r(t)$, for linearly polarized near-resonant 3 ps subcritical and super critical pump pulses which excite (a) $N_{tot}=1.63\times10^{10}$ cm^{-2} for the times $t=6$ ps (dotted line), $t=12$ ps (dashed line), and $t=20$ ps (solid line) and (b) $N_{tot}=4.63\times10^{10}$ cm^{-2} for $t=4$ ps (dotted line), $t=9$ ps (dashed line), and $t=20$ ps (solid line), respectively

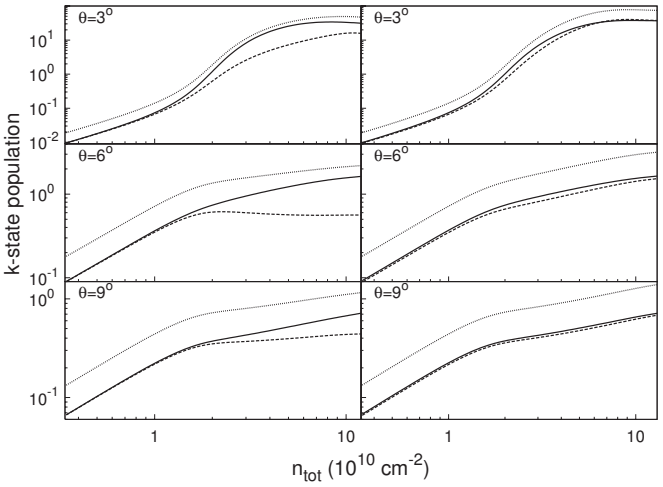

FIG. 9. Calculated populations f_k as a function of the total number of excited p's n_{tot} for three momentum states which correspond to the emission angles θ=3°, 6°, and 9° for circularly polarized pumping (left figures) and for linearly polarized pumping (right figures). Cocircular polarization: full lines, cross-circular polarization: dashed lines, and total population: dotted lines.

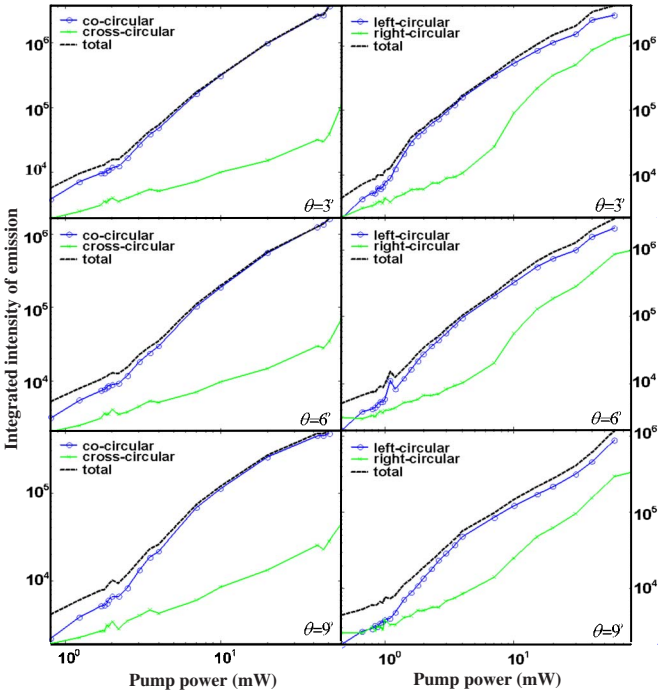

FIG. 10. (Color online) Measured pump-power dependence of the luminescence intensity for the emission angles of 3°, 6°, and 9° under circularly polarized pumping (left figures) and linearly polarized pumping (right figures) (see Ref. 23).

While the general scenario resembles the calculated ones, the differences between the measured emission of cocircular and cross-circular and right- and left-circular polarizations, respectively, are more pronounced than in the calculated results of Fig. 9. We noticed in our calculations these differences increase if the pumping gets more resonantly. On the other hand, one gets for resonant excitation a p-p scattering of two identical p's, one directly into the condensate and the other one to a higher momentum state. This results in transient nonthermal distributions in the form of an intervening accumulation of polaritons in the final high-energy state of occur. Nevertheless, the smaller calculated splittings are likely to be due to oversimplifications of the assumed cylindrical symmetry.

IV. CONCLUSIONS

Within the pseudospin formalism, we have investigated the spin and polarization kinetics as described by a 2×2 wave-number-dependent density matrix of mc p including p-phonon and p-p scattering. Using the simplifying assumption of a cylindrical symmetry, our results for circular and linear spin polarizations are in very good agreement with observations of the polarization properties of the emitted laser light. In particular, the time-averaged results of Deng *et al.*[1] for the pump-power dependence of the polarization under circularly and linearly polarized pump lights are well reproduced. The time dependence of the polarization degree measured by Renucci *et al.*[3] for various levels of resonant excitation is also reproduced qualitatively. In addition, we present calculations of the polarization of the excited p states which are found to agree at least qualitatively with the observed angle- and polarization-resolved luminescence.

ACKNOWLEDGMENTS

Two of us (H.T.C. and D.B.T.T.) gratefully acknowledge the financial support of the National Program for Basic Research. We appreciate valuable informations by Hui Deng on here angle- and polarization-resolved luminescence measurements shown in Fig. 10.

APPENDIX

In the cylindrical symmetry, the scattering terms in Eqs. (29) and (30) are given by

$$\left.\frac{\partial f_{k,i}}{\partial t}\right|_{scatt}^{p\text{-}ph} = -\frac{2\pi}{\hbar}\sum_{k'}\left[W_{k',k}f_{k,i}(1+f_{k',i}) - W_{k,k'}f_{k',i}(1+f_{k,i}) + (W_{k',k}-W_{k,k'})S_{k,k'}\right], \tag{A1}$$

$$\left.\frac{\partial S_k^r}{\partial t}\right|_{scatt}^{p\text{-}ph} = -\frac{2\pi}{\hbar}k'\left\{\left(W_{k',k}S_k^r - W_{k,k'}\frac{S_{k,k'}}{S_k^r}\right) + \frac{1}{2}(W_{k',k}-W_{k,k'})\sum_{i=1,2}\left(f_{k',i}S_k^r + f_{k,i}\frac{S_{k,k'}}{S_k^r}\right)\right\}, \tag{A2}$$

$$\left.\frac{\partial f_{k,i}}{\partial t}\right|_{scatt}^{p\text{-}p} = -\frac{2\pi}{\hbar}\sum_{k',q} V_{k'-q,k+q}^{k,k'}[f_{k,i}f_{k',i}(1+f_{k'-q,i}+f_{k+q,i}) - f_{k'-q,i}f_{k+q,i}(1+f_{k,i}+f_{k',i})]$$
$$-\frac{2\pi}{\hbar}\sum_{k',q} U_{k'-q,k+q}^{k,k'}\left\{(f_{k,i}f_{k',\bar{i}}+S_{k,k'})\left[2+\sum_{j=1,2}(f_{k'-q,j}+f_{k+q,j})\right] - (1+f_{k,i}+f_{k',\bar{i}})\left(2S_{k'-q,k+q}+\sum_{j=1,2} f_{k'-q,\bar{j}}f_{k+q,j}\right)\right\}$$
$$-\frac{2\pi}{\hbar}\sum_{k',q} T_{k'-q,k+q}^{k,k'}\left\{\sum_{j=1,2}[(f_{k',j}-f_{k'-q,j})S_{k+q,k}+(f_{k',j}-f_{k+q,j})S_{k'-q,k}] + 2[(f_{k,i}-f_{k'-q,i})S_{k+q,k'}+(f_{k,i}-f_{k+q,i})S_{k'-q,k'}]\right\}, \tag{A3}$$

$$\left.\frac{\partial S_k^r}{\partial t}\right|_{scatt}^{p\text{-}p} = -\frac{\pi}{\hbar}\sum_{k',q} V_{k'-q,k+q}^{k,k'}\left\{S_k^r\sum_{i=1,2}[f_{k',i}(1+f_{k'-q,i}+f_{k+q,i}) - f_{k'-q,i}f_{k+q,i}] - \frac{2}{S_k^r}(S_{k',k'-q}^{k,k+q}+S_{k',k+q}^{k,k'-q}-S_{k'-q,k+q}^{k,k'})\right\}$$
$$-\frac{\pi}{\hbar}\sum_{k',q} U_{k'-q,k+q}^{k,k'}\left\{\sum_{i=1,2}\left(S_k^r f_{k',i}+\frac{S_{k,k'}}{S_k^r}f_{k,i}\right)\left[2+\sum_{i=1,2}(f_{k'-q,i}+f_{k+q,i})\right]\right.$$
$$\left.-2\left(S_k^r+\frac{S_{k,k'}}{S_k^r}\right)\left[2S_{k'-q,k+q}+\sum_{i=1,2}(f_{k'-q,i}f_{k+q,\bar{i}})\right]\right\}$$
$$-\frac{\pi}{\hbar}\sum_{k',q} T_{k'-q,k+q}^{k,k'}\left\{4S_k^r(S_{k',k'-q}+S_{k',k+q})+\frac{S_{k,k'-q}}{S_k^r}\left[\sum_{i=1,2}f_{k,i}\sum_{i=1,2}(f_{k',i}-f_{k+q,i}) - 2\sum_{i=1,2}f_{k+q,i}(1+f_{k',i})\right]\right.$$
$$\left.+\frac{S_{k,k+q}}{S_k^r}\left[\sum_{i=1,2}f_{k,i}\sum_{i=1,2}(f_{k',i}-f_{k'-q,i}) - 2\sum_{i=1,2}f_{k'-q,i}(1+f_{k',i})\right]\right\}, \tag{A4}$$

where

$$V_{k_3,k_4}^{k_1,k_2} = \delta(e_{k_4}+e_{k_3}-e_{k_2}-e_{k_1})|V(k_1,k_2,k_3,k_4)|^2,$$

$$U_{k_3,k_4}^{k_1,k_2} = \delta(e_{k_4}+e_{k_3}-e_{k_2}-e_{k_1})|U(k_1,k_2,k_3,k_4)|^2,$$

$$T_{k_3,k_4}^{k_1,k_2} = \delta(e_{k_4}+e_{k_3}-e_{k_2}-e_{k_1})T(k_1,k_2,k_3,k_4),$$

and $S_{k_1,k_2}=S_{k_1}^r S_{k_2}^r \cos 2(\widehat{k_1,k_2})$ and $S_{k_3,k_4}^{k_1,k_2}=S_{k_1,k_2}S_{k_3,k_4}$.

[1] H. Deng, G. Weihs, D. Snoke, J. Bloch, and Y. Yamamoto, Proc. Natl. Acad. Sci. U.S.A. **100**, 15318 (2003).

[2] J. Kasprzak, M. Richard, S. Kundermann, A. Baas, P. Jeanbrum, J. M. Keeling, F. M. Marchetti, M. H. Szymanska, R. Andre, J. L. Staehli, V. Savona, P. B. Littlewood, B. Devaud, and Le Si Dang, Nature (London) **443**, 409 (2006).

[3] P. Renucci, T. Amand, X. Marie, P. Senellart, J. Bloch, B. Sermage, and K. V. Kavokin, Phys. Rev. B **72**, 075317 (2005).

[4] I. A. Shelykh, A. V. Kavokin, and G. Malpuech, Phys. Status Solidi B **242**, 2271 (2005).

[5] I. A. Shelykh, K. V. Kavokin, A. V. Kavokin, G. Malpuech, P. Biegenwald, H. Deng, G. Weihs, and Y. Yamamoto, Phys. Rev. B **70**, 035320 (2004).

[6] D. N. Krizhanovskii, D. Sanvitto, I. A. Shelykh, M. M. Glazov, G. Malpuech, D. D. Solnyshkov, A. Kavokin, S. Ceccarelli, M. S. Skolnick, and J. S. Roberts, Phys. Rev. B **73**, 073303 (2006).

[7] D. D. Solnyshkov, I. A. Shelykh, M. M. Glazov, G. Malpuech, T. Amand, P. Renucci, X. Marie, and A. V. Kavokin, Semiconductors **42**, 1099 (2007).

[8] H. Haug and S. W. Koch, *Quantum Theory of the Optical and Electronic Properties of Semiconductors* (World Scientific, Singapore, 2004).

[9] K. V. Kavokin, I. A. Shelykh, A. V. Kavokin, G. Malpuech, and P. Bigenwald, Phys. Rev. Lett. **92**, 017401 (2004).

[10] H. T. Cao, T. D. Doan, D. B. Tran Thoai, and H. Haug, Phys. Rev. B **69**, 245325 (2004).

[11] T. D. Doan, H. T. Cao, D. B. Tran Thoai, and H. Haug, Phys. Rev. B **72**, 085301 (2005).

[12] T. D. Doan, H. T. Cao, D. B. Tran Thoai, and H. Haug, Phys. Rev. B **74**, 115316 (2006).

[13] R. Graham and A. Wunderlin, *Lasers and Synergetics* (Springer, Berlin, 1987).

[14] I. Shelykh, G. Malpuech, K. V. Kavokin, A. V. Kavokin, and P. Bigenwald, Phys. Rev. B **70**, 115301 (2004).

[15] L. Klopotovski, M. D. Martin, A. Amo, L. Vina, I. A. Shelykh, M. M. Glazov, G. Malpuech, A. V. Kavokin, and R. Andre, Solid State Commun. **139**, 511 (2006).
[16] C. Piermarocchi, F. Tassone, V. Savona, A. Quattropani, and P. Schwendimann, Phys. Rev. B **53**, 15834 (1996).
[17] A. Kavokin, G. Malpuech, and M. Glazov, Phys. Rev. Lett. **95**, 136601 (2005).
[18] J. Bloch and J. Y. Marzin, Phys. Rev. B **56**, 2103 (1997).
[19] F. Tassone, C. Piermarocchi, V. Savona, A. Quattropani, and P. Schwendimann, Phys. Rev. B **56**, 7554 (1997).
[20] L. Banyai, P. Gartner, O. M. Schmitt, and H. Haug, Phys. Rev. B **61**, 8823 (2000).
[21] S. Pau, G. Bjork, J. Jacobson, H. Cao, and Y. Yamamoto, Phys. Rev. B **51**, 7090 (1995).
[22] U. Bockelmann, Phys. Rev. B **48**, R17637 (1993).
[23] H. Deng, G. Weihs, D. Snoke, J. Bloch, and Y. Yamamoto (unpublished).